

Joint Network-and-Server Congestion in Multi-Source Traffic Allocation: A Convex Formulation and Price-Based Decentralization

Tamoghna Sarkar and Bhaskar Krishnamachari

Ming Hsieh Department of Electrical and Computer Engineering

Viterbi School of Engineering, University of Southern California

Los Angeles, CA, USA

{tsarkar, bkrishna}@usc.edu

Abstract—This paper studies an important rate allocation problem that arises in many networked and distributed systems: steady-state traffic rate allocation from multiple sources to multiple service nodes when both (i) the access-path delay on each source-node route is rate-dependent (capacity-constrained) and convex, and (ii) each service node (also capacity-constrained) experiences a load-dependent queueing delay driven by aggregate load from all sources. We show that the resulting flow-weighted end-to-end delay minimization is a convex program, yielding a global system-optimal solution characterized by KKT conditions that equalize total marginal costs (a path marginal access term plus a node congestion price) across all utilized routes. This condition admits a Wardrop-type interpretation: for each source, all utilized options equalize total marginal cost, while any option with strictly larger total marginal cost receives no flow. Building on this structure, we develop a lightweight distributed pricing-based algorithm in which each service node locally computes and broadcasts a scalar congestion price from its observed aggregate load, while each source updates its traffic split by solving a small separable convex allocation problem under the advertised prices. Numerical illustrations demonstrate convergence of the distributed iteration to the centralized optimum and highlight the trade-offs induced by jointly modeling access and service congestion.

Index Terms—rate allocation, traffic allocation, convex optimization, queueing delay, load balancing, marginal cost pricing, Wardrop condition, distributed algorithm

I. INTRODUCTION

Many networked systems route traffic from multiple ingress points to one of several service nodes (often with splittable flow), including edge-to-cloud offloading, pub-sub overlays with distributed brokers, and wireless/RAN traffic steering across base stations or compute pools. A recurring difficulty is that end-to-end latency is shaped by *two coupled congestion effects*: (i) the access path from a source to a chosen node can become congested as more rate is routed on that path, and (ii) the service node itself incurs queueing/processing delay that grows with aggregate load. Steering traffic to a nearby node may reduce baseline transport delay but overload either the access path or the node; steering to a lightly-loaded node may reduce server delay but increase access delay. These access-service trade-offs motivate allocation mechanisms that

are globally optimal under clear conditions yet implementable with lightweight distributed signaling.

Model overview: We study a steady-state allocation problem with sources $i \in \mathcal{I}$ of fixed offered rates λ_i that split traffic across service nodes $j \in \mathcal{J}$ via $\lambda_{ij} \geq 0$. Traffic on (i, j) experiences an increasing convex *rate-dependent access delay* $D_{ij}(\lambda_{ij})$, while service node j experiences an increasing convex *load-dependent delay* $D_j(\Lambda_j)$ under aggregate load $\Lambda_j = \sum_i \lambda_{ij}$. Our objective minimizes total flow-weighted end-to-end delay (formalized in Sec. III), yielding a convex program under standard assumptions. This convexity enables a transparent optimality characterization in terms of *total marginal cost* equalization.

II. RELATED WORK

The problem of allocating traffic across heterogeneous resources sits at the intersection of network utility maximization, distributed load balancing, and modern radio access network (RAN) control. We categorize related literature into three primary domains.

A. Theoretical Foundations and Pricing

The foundational framework for distributed delay minimization was established by Gallager, who derived necessary conditions for optimal routing based on marginal delay equalization [1]. This gradient-based approach was later generalized into the Network Utility Maximization (NUM) framework by Kelly *et al.* [2] and Low *et al.* [3], which interprets congestion signals as shadow prices to coordinate source rates.

While these works primarily focus on transport capacity, recent economic interpretations have bridged the gap between user equilibrium and system optimality. Rambha *et al.* [4] demonstrated that marginal cost pricing is the necessary mechanism to align selfish routing with global system optima in transportation networks. From a game-theoretic perspective, Paccagnan *et al.* [5] characterize the relationship between Nash and Wardrop equilibria in aggregative games with coupling constraints and propose decentralized algorithms that converge to these equilibrium notions, providing useful context for Wardrop-type interpretations under shared constraints.

Our work extends these ideas by introducing a joint cost model that couples rate-dependent access delays with load-dependent server queueing delays and yields a Wardrop-type total marginal-cost equalization condition on a bipartite source-server topology.

Complementary to our model-based approach, Vu *et al.* [6] study fast routing under uncertainty via adaptive learning in (nonatomic) congestion games with exponential weights, offering a learning-theoretic viewpoint on routing dynamics when costs fluctuate or are only observed implicitly.

B. Wireless and O-RAN Traffic Steering

In the context of 5G/6G and Open RAN (O-RAN), traffic steering is often treated as a complex resource management problem. Nguyen *et al.* proposed a multi-layer optimization framework for O-RAN that accounts for interference and functional splits, though the resulting non-convexity requires computationally intensive solutions [7]. Conversely, data-driven approaches, such as the Deep Reinforcement Learning (DRL) steering mechanisms proposed by Habib *et al.* [8], offer flexibility against unknown network dynamics but lack interpretability and provable convergence guarantees.

Our approach offers a middle ground: a convex “white-box” formulation that retains the lightweight signaling of heuristic methods: broadcasting a single scalar price per server. This makes it highly suitable for the bandwidth-constrained E2 interface in O-RAN architectures.

C. Edge Computing and Load Balancing

In distributed computing, load balancing strategies have evolved from queue-length-based heuristics, such as the “Power of Two Choices” [9] and Join-Idle-Queue (JIQ) [10], to more rigorous optimization methods. While heuristics are asymptotically optimal in large-scale homogeneous systems, they often struggle with the heterogeneity inherent in edge-cloud continuums.

In large operational networks, PLB [11] demonstrates that simple congestion signals can be highly effective for load balancing by triggering path changes in response to congestion, supporting the broader premise that lightweight scalar signals can coordinate distributed traffic allocation. Recent work by Balseiro *et al.* [12] addresses heterogeneity by applying distributed gradient descent to load balancing with network latencies, a model closely related to ours, though their focus lies heavily on stability analysis under delayed feedback. Similarly, Urgaonkar *et al.* [13] employed Lyapunov optimization for dynamic workload scheduling, and Nguyen *et al.* [14] explored market-equilibrium approaches for fair resource sharing among competing slices. In contrast, our work prioritizes the minimization of total flow-weighted system delay through a unified marginal cost structure, providing a centralized benchmark and a convergent distributed pricing algorithm.

D. Motivating applications

Although the formulation in this paper is intentionally abstract, it captures a common set of trade-offs across many

practical systems. We highlight four motivating examples to illustrate the generality of this formulation, including wireless-network scenarios.

a) Traffic steering and load balancing across small cells in dense wireless HetNets: In dense 5G and 6G deployments, traffic aggregates, or UEs and gateways, can be steered toward different candidate base stations, such as macro cells and small cells, or toward different sectors. Here, $D_{ij}(\lambda_{ij})$ can represent an access-side delay that grows with the offered load on the chosen radio and backhaul route, while $D_j(\Lambda_j)$ captures scheduling or queueing delay that rises as a cell or compute pool approaches saturation.

b) Cloud-RAN and vRAN processing allocation across DU and CU pools: In virtualized RAN architectures, radio units (sources) may send baseband workloads to one of several DU and CU pools or accelerator clusters (servers) over fronthaul and midhaul. The function $D_{ij}(\lambda_{ij})$ captures load-dependent transport or buffering delay on the corresponding fronthaul/midhaul path, while $D_j(\Lambda_j)$ captures compute queueing or processing delay at pool j driven by aggregate workload.

c) Pub-Sub traffic allocation across geographically distributed brokers: Publishers (sources) such as IoT devices may route messages to one of several brokers (servers) that differ in network distance and in access-path conditions. The function $D_{ij}(\lambda_{ij})$ captures publisher-to-broker access delay that increases as more traffic is routed along that path (e.g., due to ingress bottlenecks or intermediate queues), while $D_j(\Lambda_j)$ captures broker queueing or processing delay as aggregate publish rate Λ_j grows.

d) Edge-to-cloud offloading across multiple compute sites: Edge nodes (sources) offload tasks to a set of cloud or edge data centers (servers). The function $D_{ij}(\lambda_{ij})$ captures uplink and transport delay that can increase with the offered rate on the selected access route, while $D_j(\Lambda_j)$ captures compute queueing delay at site j driven by aggregate offloaded workload.

These examples share a common optimization structure and tradeoff: Traffic should be directed to favorable access paths when possible, but must also be distributed to prevent both access bottlenecks and overloaded service nodes from dominating end-to-end latency. We hasten to add that the problem being addressed in this paper is not at all artificial. In fact, we originally formulated it in the context of one of the above distributed system applications (specifically, pub-sub traffic allocation) to address a practical concern encountered in an industrial setting. Stepping back, we could see its much broader applicability in the other applications, including in the context of wireless networks, as noted above.

E. Results and contributions

This paper provides both centralized and distributed methods for solving (4). First, we characterize the globally optimal allocation via convex optimization and KKT conditions, which yields a clear *total marginal cost* structure. Servers used by a given source equalize the sum of a path-dependent marginal

access term and a server-dependent marginal congestion price. This structural view leads to a pricing interpretation: Each service node computes and broadcasts a scalar congestion price as a function of its current aggregate load. Second, we develop a lightweight distributed algorithm based on this interpretation. Service nodes iteratively update and broadcast their congestion prices, and sources update their traffic splits by solving small separable convex allocation problems under the advertised prices. The algorithm requires minimal signaling, since each service node broadcasts a single scalar per iteration. Under standard stepsize conditions, the distributed dynamics converge to the centralized optimum.

While the algorithmic mechanics leverage established principles of network utility maximization and pricing-based distributed iteration, the distinct contribution of this work is the structural synthesis of rate-dependent access delays and load-dependent service delays into a unified framework. This formulation yields three specific benefits over generic optimization approaches: 1) it captures the specific architectural constraints of modern edge, O-RAN and cloud distributed systems where access and compute bottlenecks are coupled; 2) it demonstrates that a single scalar price is sufficient to coordinate this joint problem, offering a highly interpretable control plane; and 3) it provides a provably optimal benchmark against which domain-specific heuristic load-balancing strategies can be rigorously evaluated.

F. Paper organization

The remainder of the paper is organized as follows. Section III describes the system model and formalizes the traffic allocation problem. Section IV analyzes the convex program, derives the optimality conditions, and presents the centralized solution characterization. Section V introduces the distributed price-based algorithm and discusses its convergence properties. Section VI provides numerical illustrations demonstrating the effectiveness of the proposed approach under representative parameter settings. Finally, Section VII concludes and outlines directions for future work.

III. SYSTEM MODEL AND PROBLEM FORMULATION

We consider a system with multiple independent traffic sources and multiple service nodes (SN). The model represents a steady-state load allocation problem in which traffic from multiple sources is routed to heterogeneous service nodes with finite capacities. The delay here consists of a path-dependent queueing component that depends on the traffic placed on each source to service-node path and the traffic arriving to a service-node queueing component that depends on aggregate load at each SN.

A. System Model

Let $\mathcal{I} = \{1, \dots, m\}$ denote the set of traffic sources and $\mathcal{J} = \{1, \dots, n\}$ the set of service nodes. Each source $i \in \mathcal{I}$ generates traffic at a fixed rate $\lambda_i > 0$. Traffic from a source may be split arbitrarily across service nodes. Let $\lambda_{ij} \geq 0$

denote the rate at which source i sends traffic to service node j .

The routing variables $\{\lambda_{ij}\}$ are the decision variables of the system and satisfy the flow conservation constraints for each source i : $\sum_{j \in \mathcal{J}} \lambda_{ij} = \lambda_i$. Each source-node path (i, j) is associated with a finite access capacity $\mu_{ij} > 0$. We restrict attention to feasible operating points satisfying $\lambda_{ij} < \mu_{ij}$ for all (i, j) . This captures access bottlenecks such as last-mile links, ingress queues, or admission limits that become unstable as the routed rate approaches μ_{ij} .

Each service node $j \in \mathcal{J}$ provides service at rate $\mu_j > 0$. The aggregate arrival rate at node j is specified as: $\Lambda_j \triangleq \sum_{i \in \mathcal{I}} \lambda_{ij}$, which must satisfy a stability condition $\Lambda_j < \mu_j$.

B. Delay Model

Traffic routed from source i to service node j experiences two queueing components.

a) *Path-dependent access delay*: Let $D_{ij}(\cdot)$ denote the access (or path) delay function on the route from source i to service node j , modeled as a function of the routed rate λ_{ij} . We assume $D_{ij}(\lambda_{ij})$ is continuous, twice-differentiable, strictly increasing, and convex over the domain $\lambda_{ij} < \mu_{ij}$, and satisfies $\lim_{\lambda_{ij} \uparrow \mu_{ij}} D_{ij}(\lambda_{ij}) = +\infty$.

A canonical example is the M/M/1 access-delay model,

$$D_{ij}(\lambda_{ij}) = \frac{1}{\mu_{ij} - \lambda_{ij}}. \quad (1)$$

Our analysis applies to any access delay function satisfying the above properties.

b) *SN queueing delay*: Let $D_j(\cdot)$ denote the queueing delay function at service node j , which depends on the aggregate arrival rate. We model the queueing delay at service node j as a function $D_j(\Lambda_j)$ that is continuous, twice-differentiable, strictly increasing, and convex over the domain $\Lambda_j < \mu_j$. A canonical example is the M/M/1 model

$$D_j(\Lambda_j) = \frac{1}{\mu_j - \Lambda_j}. \quad (2)$$

though our analysis applies to any delay function satisfying the above properties.

c) *End-to-end delay*: The total end-to-end delay experienced by traffic from source i to service node j is

$$\tilde{D}_{ij}(\lambda) = D_{ij}(\lambda_{ij}) + D_j(\Lambda_j). \quad (3)$$

C. Optimization Objective

Given the system model and delay structure described above, traffic routed from source i to service node j experiences an end-to-end delay $\tilde{D}_{ij}(\lambda)$. The system-wide performance depends on how traffic is split across service nodes and on the access and SN queueing delays induced by the resulting routed and aggregate loads. We therefore consider an objective that minimizes the total delay experienced by all traffic in the system, weighted by the corresponding flow rates.

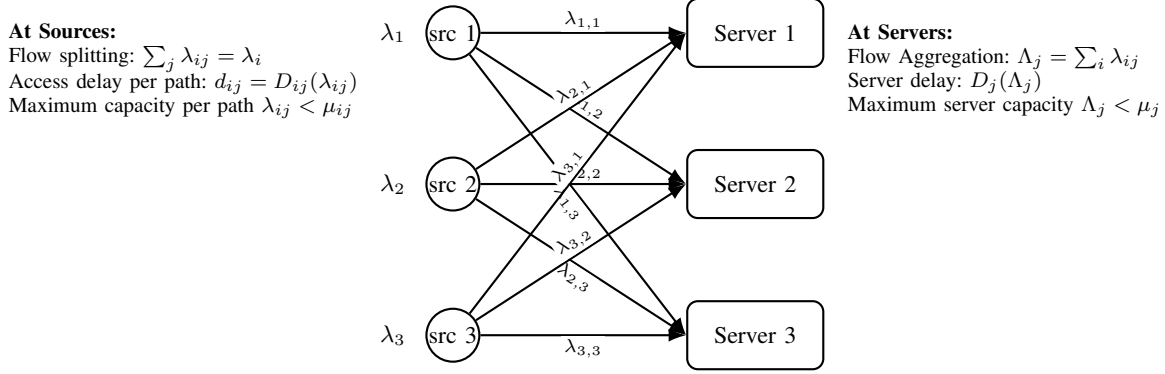


Fig. 1. Illustration of the general formulation (paper notation). Each source i with rate λ_i splits traffic into λ_{ij} over servers j . Each path has capacity μ_{ij} and experiences a convex increasing access delay $D_{ij}(\lambda_{ij})$. Each server j experiences load $\Lambda_j = \sum_i \lambda_{ij}$ and a convex increasing delay $D_j(\Lambda_j)$, with capacity μ_j .

Formally, we consider the following optimization problem: and for each service node j , define

$$\min_{\{\lambda_{ij}\}} \sum_{i \in \mathcal{I}} \sum_{j \in \mathcal{J}} \lambda_{ij} \tilde{D}_{ij}(\lambda) \quad (4)$$

$$\text{s.t. } \sum_{j \in \mathcal{J}} \lambda_{ij} = \lambda_i, \quad \forall i \in \mathcal{I}, \quad (5)$$

$$\lambda_{ij} \geq 0, \quad \forall i \in \mathcal{I}, j \in \mathcal{J}, \quad (6)$$

$$\sum_{i \in \mathcal{I}} \lambda_{ij} \leq \mu_j - \epsilon, \quad \forall j \in \mathcal{J}, \quad (7)$$

$$\lambda_{ij} \leq \mu_{ij} - \epsilon, \quad \forall i \in \mathcal{I}, j \in \mathcal{J} \quad (8)$$

This objective captures the aggregate delay experienced by all traffic in the system and defines a system-optimal routing policy. Under the stated assumptions on the delay functions $D_{ij}(\cdot)$ and $D_j(\cdot)$, the problem is convex in the routing variables over the feasible region, as established in the next section.

IV. CENTRALIZED SYSTEM-OPTIMAL SOLUTION

We next characterize the structure of the system-optimal solution under centralized control for the formulation in Section III, in which end-to-end delay includes both a path-dependent access delay that depends on λ_{ij} and a SN queueing delay that depends on Λ_j .

A. Convexity and Existence

We establish convexity of the optimization problem (4) by rewriting the objective as a sum of separable convex terms. Recalling that $\tilde{D}_{ij}(\lambda) = D_{ij}(\lambda_{ij}) + D_j(\Lambda_j)$ and $\Lambda_j = \sum_{i \in \mathcal{I}} \lambda_{ij}$, the objective can be expressed as

$$\begin{aligned} \sum_{i \in \mathcal{I}} \sum_{j \in \mathcal{J}} \lambda_{ij} \tilde{D}_{ij}(\lambda) &= \sum_{i \in \mathcal{I}} \sum_{j \in \mathcal{J}} \lambda_{ij} D_{ij}(\lambda_{ij}) + \sum_{i \in \mathcal{I}} \sum_{j \in \mathcal{J}} \lambda_{ij} D_j(\Lambda_j) \\ &= \sum_{i \in \mathcal{I}} \sum_{j \in \mathcal{J}} \lambda_{ij} D_{ij}(\lambda_{ij}) + \sum_{j \in \mathcal{J}} \Lambda_j D_j(\Lambda_j). \end{aligned} \quad (9)$$

For each pair (i, j) , define

$$g_{ij}(x) \triangleq x D_{ij}(x), \quad x < \mu_{ij},$$

Under the assumptions in Section III, $D_{ij}(\cdot)$ is continuous, strictly increasing, convex, and differentiable on $x < \mu_{ij}$, and similarly $D_j(\cdot)$ is continuous, strictly increasing, convex, and differentiable on $x < \mu_j$. It follows that

$$\begin{aligned} g_{ij}''(x) &= 2D'_{ij}(x) + x D''_{ij}(x) \geq 0, \\ g_j''(x) &= 2D'_j(x) + x D''_j(x) \geq 0. \end{aligned}$$

so $g_{ij}(\cdot)$ is convex on $x < \mu_{ij}$ and $g_j(\cdot)$ is convex on $x < \mu_j$. Since each λ_{ij} enters the first term of (9) through the convex function $g_{ij}(\lambda_{ij})$, the access-delay component is convex in $\{\lambda_{ij}\}$. Moreover, each aggregate arrival rate Λ_j is an affine function of $\{\lambda_{ij}\}_{i \in \mathcal{I}}$, so the composition $g_j(\Lambda_j) = \Lambda_j D_j(\Lambda_j)$ is convex in the routing variables. Summing convex terms preserves convexity, implying that the objective in (4) is convex in $\{\lambda_{ij}\}$ over the feasible region.

The feasible set defined by the flow conservation, non-negativity, and stability constraints is convex. For queueing delay models of interest, including the M/M/1 form in (1) and (2), the terms $g_{ij}(\lambda_{ij})$ and $g_j(\Lambda_j)$ diverge as $\lambda_{ij} \uparrow \mu_{ij}$ and $\Lambda_j \uparrow \mu_j$, respectively, ensuring that any minimizing sequence remains strictly within the stability region. Therefore, the optimization problem (4) admits an optimal solution.

Because the objective is convex and the constraints are affine, the Karush-Kuhn-Tucker (KKT) conditions are both necessary and sufficient for global optimality. In the next subsection, we use these conditions to characterize the structure of the system-optimal routing policy.

B. Optimality Conditions and Structural Properties

We now characterize the structure of the system-optimal solution by deriving the KKT conditions. These conditions yield an interpretation of optimal routing in terms of *total marginal delay costs* that include both access and SN congestion effects.

Lagrangian and KKT Conditions: Let α_i denote the Lagrange multiplier associated with the flow conservation constraint $\sum_{j \in \mathcal{J}} \lambda_{ij} = \lambda_i$ for source i , and let $\beta_{ij} \geq 0$ denote the multiplier associated with the non-negativity constraint $\lambda_{ij} \geq 0$. (We treat the strict stability constraints $\lambda_{ij} < \mu_{ij}$ and $\Lambda_j < \mu_j$ as part of the domain; for the queueing models of interest the objective diverges at the boundary, so the optimum lies in the interior.)

The Lagrangian is given by

$$\begin{aligned} \mathcal{L}(\lambda, \alpha, \beta) = & \sum_{i \in \mathcal{I}} \sum_{j \in \mathcal{J}} \lambda_{ij} D_{ij}(\lambda_{ij}) + \sum_{j \in \mathcal{J}} \Lambda_j D_j(\Lambda_j) \\ & + \sum_{i \in \mathcal{I}} \alpha_i \left(\lambda_i - \sum_{j \in \mathcal{J}} \lambda_{ij} \right) - \sum_{i \in \mathcal{I}} \sum_{j \in \mathcal{J}} \beta_{ij} \lambda_{ij}, \end{aligned} \quad (10)$$

where $\Lambda_j = \sum_{i \in \mathcal{I}} \lambda_{ij}$.

Stationarity with respect to λ_{ij} yields

$$\begin{aligned} & \left[D_{ij}(\lambda_{ij}) + \lambda_{ij} D'_{ij}(\lambda_{ij}) \right] + \left[D_j(\Lambda_j) + \Lambda_j D'_j(\Lambda_j) \right] \\ & - \alpha_i - \beta_{ij} = 0, \quad \forall i, j. \end{aligned} \quad (11)$$

Together with primal feasibility, dual feasibility $\beta_{ij} \geq 0$, and complementary slackness

$$\beta_{ij} \lambda_{ij} = 0,$$

these conditions fully characterize the system-optimal solution.

Total Marginal Delay Equalization: Define the *marginal access cost* on path (i, j) as

$$C_{ij}(\lambda_{ij}) \triangleq D_{ij}(\lambda_{ij}) + \lambda_{ij} D'_{ij}(\lambda_{ij}), \quad (12)$$

and define the *marginal SN congestion cost* at node j as

$$C_j(\Lambda_j) \triangleq D_j(\Lambda_j) + \Lambda_j D'_j(\Lambda_j). \quad (13)$$

The stationarity condition (11) can then be written as

$$C_{ij}(\lambda_{ij}) + C_j(\Lambda_j) \begin{cases} = \alpha_i, & \text{if } \lambda_{ij} > 0, \\ \geq \alpha_i, & \text{if } \lambda_{ij} = 0. \end{cases} \quad (14)$$

Equation (14) implies that, at optimality, each source i routes traffic only over source-node paths (i, j) that minimize the *sum of marginal access cost and marginal SN congestion cost*. All service nodes that receive positive traffic from a given source i have equal total marginal cost $C_{ij}(\lambda_{ij}) + C_j(\Lambda_j)$, while unused paths incur no smaller total marginal cost.

Wardrop-type Interpretation: The condition (14) admits a Wardrop-type interpretation in terms of *total marginal costs*. For a given source, all utilized options equalize total marginal cost, while any option with strictly larger total marginal cost receives no flow. This equalization arises as a consequence of system-optimal routing for a convex objective, without invoking any equilibrium or selfish-routing assumptions.

We treat this centralized solution as a full-information benchmark, against which decentralized implementation can be compared. The marginal-cost structure in (14) will also serve as the basis for the distributed pricing-based solution developed in the next section.

V. DISTRIBUTED PRICING-BASED SOLUTION

Section IV shows that the system-optimal allocation can be expressed through *total marginal costs*: a path-dependent marginal access term and a service-node (SN) marginal congestion term. We now leverage this structure to obtain a distributed method that achieves the same optimum without a central coordinator. Each SN computes and broadcasts a scalar congestion *price* from its locally observed aggregate load, and each source updates its traffic split by solving a small convex subproblem using locally known access-delay functions and the advertised prices.

A. Pricing interpretation

From the centralized KKT conditions in Section IV-B, optimality requires total marginal-cost equalization across the options used by each source; see (14). This suggests the following decentralization: define the congestion *price* at SN j as the marginal congestion cost (13), which depends only on the aggregate load at j and is therefore locally computable. Given advertised prices, the remaining marginal access term is local to each source-path pair, so sources can update their allocations using only $(\lambda_i, \{D_{ij}\}_j)$ and the received price vector.

B. Source routing update

Given prices p , each source i computes a best-response routing vector by solving the separable convex subproblem in Algorithm 1.

To avoid overly aggressive simultaneous reactions to changing prices, sources apply a damped update as shown in Algorithm 1, which preserves feasibility by construction.

C. Service-node price update

Each SN j measures its aggregate arrival rate and computes the induced instantaneous marginal congestion cost. For stability under simultaneous source updates and noisy load estimates, SNs apply the damped price update (see Algorithm 1) and broadcast the resulting scalar prices to all sources.

D. Distributed Algorithm

Algorithm 1 requires only scalar signaling from SNs: each SN broadcasts a single price $p_j^{(t)}$ per iteration, computed from its locally observed load. Sources then update by (damped) best responses to the received prices. At any fixed point, the induced allocations satisfy the total marginal-cost equalization condition (14) and therefore coincide with the centralized optimum.

Assumption: Algorithm 1 is analyzed on the feasible set $\{\lambda : \Lambda_j < \mu_j, \lambda_{ij} < \mu_{ij}\}$.

E. Implementation considerations

The method is implementable with local measurements at SNs and limited signaling. Each SN needs only its aggregate arrival-rate estimate to compute and publish a scalar price; it need not track per-source contributions. Each source needs only its own offered rate and access-delay models (or marginal

Algorithm 1: Distributed Pricing-Based Routing with Path-Dependent Access Delays

```

Input: rates  $\{\lambda_i\}$ , access delay functions  $\{D_{ij}(\cdot)\}$ ,  

       service delay functions  $\{D_j(\cdot)\}$ , stepsizes  

        $\{\eta_t\}, \{\gamma_t\}$  with  $\eta_t, \gamma_t \in (0, 1]$ 
Input: initialize feasible routing  $\{\lambda_{ij}^{(0)}\}$  and prices  

        $\{p_j^{(0)}\}$ 
1 for  $t \leftarrow 0, 1, 2, \dots$  do
    // Service-node price update
    // (local)
    2 foreach  $j \in \mathcal{J}$  do
        3  $\Lambda_j^{(t)} \leftarrow \sum_{i \in \mathcal{I}} \lambda_{ij}^{(t)}$ 
        4  $\hat{p}_j^{(t)} \leftarrow D_j(\Lambda_j^{(t)}) + \Lambda_j^{(t)} D'_j(\Lambda_j^{(t)})$ 
        5  $p_j^{(t+1)} \leftarrow (1 - \gamma_t) p_j^{(t)} + \gamma_t \hat{p}_j^{(t)}$ 
    // Broadcast prices
    6 broadcast  $\{p_j^{(t+1)}\}_{j \in \mathcal{J}}$  to all sources
    // Source routing update (local
    // convex subproblem)
    7 foreach  $i \in \mathcal{I}$  do
        8 compute best responses  $\lambda_{ij}^{\text{br}}(\mathbf{p}^{(t+1)})$  by solving
            
$$\min_{\{\lambda_{ij}\}_{j \in \mathcal{J}}} \sum_{j \in \mathcal{J}} \left( \lambda_{ij} D_{ij}(\lambda_{ij}) + p_j^{(t+1)} \lambda_{ij} \right)$$

            s.t.  $\sum_{j \in \mathcal{J}} \lambda_{ij} = \lambda_i, \quad \lambda_{ij} \geq 0;$ 
            9  $\lambda_{ij}^{(t+1)} \leftarrow (1 - \eta_t) \lambda_{ij}^{(t)} + \eta_t \lambda_{ij}^{\text{br}}(\mathbf{p}^{(t+1)})$ 
    // Stopping criterion (optional)
    10 if  $\|\lambda^{(t+1)} - \lambda^{(t)}\| \leq \varepsilon$  then
        break

```

access costs) to solve its local subproblem under the advertised prices.

Algorithm 1 is written in synchronous rounds for clarity. The same updates can be implemented asynchronously by having SNs refresh prices on load changes and sources update upon receiving new prices; in that case, stale prices can be handled via smaller stepsizes or additional damping. A detailed treatment of delayed and time-varying implementations is left for future work.

F. Convergence Properties

Fixed points, convergence, and optimality: A fixed point of Algorithm 1 is a pair $(\lambda^*, \mathbf{p}^*)$ such that the induced loads $\Lambda_j^* = \sum_i \lambda_{ij}^*$ satisfy

$$p_j^* = D_j(\Lambda_j^*) + \Lambda_j^* D'_j(\Lambda_j^*), \quad \forall j \in \mathcal{J}, \quad (15)$$

and each source i is optimal for its local subproblem under prices \mathbf{p}^* . Equivalently, for each $i \in \mathcal{I}$ there exists a scalar α_i^* such that

$$C_{ij}(\lambda_{ij}^*) + p_j^* \begin{cases} = \alpha_i^*, & \text{if } \lambda_{ij}^* > 0, \\ \geq \alpha_i^*, & \text{if } \lambda_{ij}^* = 0, \end{cases} \quad \forall j \in \mathcal{J}, \quad (16)$$

where $C_{ij}(\lambda) = D_{ij}(\lambda) + \lambda D'_j(\lambda)$.

Standing conditions: Throughout, we restrict attention to feasible iterates and assume $\Lambda_j^{(t)} < \mu_j$ and $\lambda_{ij}^{(t)} < \mu_{ij}$ for all j and all (i, j) . Let the stepsizes satisfy $\eta_t, \gamma_t \in (0, 1]$ and the standard diminishing conditions $\sum_{t=0}^{\infty} \eta_t = \infty$, $\sum_{t=0}^{\infty} \eta_t^2 < \infty$, and similarly $\sum_{t=0}^{\infty} \gamma_t = \infty$, $\sum_{t=0}^{\infty} \gamma_t^2 < \infty$. Define $\hat{p}(\lambda)$ by (15) and let $\text{BR}(p)$ denote the concatenation of per-source minimizers of the subproblem in Algorithm 1. Assume the induced fixed-point map $T(\lambda, p) \triangleq (\text{BR}(p), \hat{p}(\lambda))$ is a contraction on the feasible set.

Theorem (Convergence and optimality of Algorithm 1) Algorithm 1 converges to a fixed point $(\lambda^*, \mathbf{p}^*)$, where λ^* is a system-optimal routing solution of (4).

Proof. Due to page limitations, we sketch the proof here. A longer version of this paper with the full proof will be posted online on arXiv. Algorithm 1 implements a relaxed fixed-point iteration toward T : the price update is $p^{(t+1)} = (1 - \gamma_t) p^{(t)} + \gamma_t \hat{p}(\lambda^{(t)})$ and the source update is $\lambda^{(t+1)} = (1 - \eta_t) \lambda^{(t)} + \eta_t \text{BR}(p^{(t+1)})$.

Under the contraction assumption on T and the diminishing stepsizes, Algorithm 1 implements a relaxed fixed-point iteration toward T . Standard convergence results for such iterations imply $(\lambda^{(t)}, p^{(t)}) \rightarrow (\lambda^*, \mathbf{p}^*)$ with $(\lambda^*, \mathbf{p}^*) = T(\lambda^*, \mathbf{p}^*)$.

Finally, any fixed point is globally optimal for (4). By (15), $p_j^* = C_j(\Lambda_j^*) = D_j(\Lambda_j^*) + \Lambda_j^* D'_j(\Lambda_j^*)$. By (16), for each source i there exists α_i^* such that $C_{ij}(\lambda_{ij}^*) + p_j^* = \alpha_i^*$ if $\lambda_{ij}^* > 0$ and $C_{ij}(\lambda_{ij}^*) + p_j^* \geq \alpha_i^*$ if $\lambda_{ij}^* = 0$. Substituting $p_j^* = C_j(\Lambda_j^*)$ recovers the KKT marginal-cost equalization conditions derived in Section IV-B. Since (4) is a convex program with affine constraints, KKT implies global optimality, hence λ^* is system-optimal.

VI. ILLUSTRATIVE RESULTS

This section presents a synthetic numerical illustration of the proposed convex flow-weighted allocation objective and the distributed pricing-based iteration on a static multi-source, multi-server topology with heterogeneous access capacities and server service rates. The purpose is to (i) verify feasibility and convergence behavior of the distributed dynamics, and (ii) quantify how closely the distributed solution matches the centralized optimum.

A. Experimental Setup

We evaluate the centralized flow-weighted optimum and the distributed pricing-based iteration on a fixed (static) instance with heterogeneous source rates and heterogeneous access/server capacities. The goal is purely illustrative: to verify convergence of the distributed pricing iteration to the centralized convex optimum under the joint access-and-service congestion model.

a) Static instance: We use one static routing instance with $m = 5$ sources and $n = 3$ service nodes. We evaluate the flow-weighted objective in (4) using delay functions for $D_{ij}(\lambda_{ij})$ and $D_j(\Lambda_j)$.

b) *Arrival rates*: To obtain heterogeneous source rates, we define four traffic classes with fixed message rates and mean sizes: class 1 is 50 msg/s at 2 KB, class 2 is 30 msg/s at 2 KB, class 3 is 15 msg/s at 2 MB, and class 4 is 10 msg/s at 1 KB. Each source i is assigned a fixed subset of classes, and its exogenous rate λ_i is computed by summing the corresponding byte rates and converting to MB/s. The resulting vector $\lambda = (\lambda_i)_{i \in \mathcal{I}}$ is held fixed for both solvers.

c) *Access and service capacities*: The access capacities $\{\mu_{ij}\}$ and service capacities $\{\mu_j\}$ are fixed heterogeneous values for this instance and define the stability domain conditions.

d) *Initialization*: Both solvers start from a strictly feasible allocation that satisfies $\sum_j \lambda_{ij} = \lambda_i$ for all sources, respects the access bounds $\lambda_{ij} \leq \mu_{ij} - \epsilon$, and satisfies the server feasibility constraints $\sum_i \lambda_{ij} \leq \mu_j - \epsilon$ for all j , with a small $\epsilon > 0$.

e) *Centralized solver configuration*: The centralized optimum is computed by minimizing the convex objective in (4) with a constrained solver (trust-constr) using analytic gradients. The constraints enforce the row-sum equalities and the server-capacity inequalities, with bounds $0 \leq \lambda_{ij} \leq \mu_{ij} - \epsilon$.

f) *Distributed solver configuration and stopping criterion*: The distributed iteration follows Algorithm 1. At each iteration, each service node updates its scalar price using the marginal congestion cost $p_j = D_j(\Lambda_j) + \Lambda_j D'_j(\Lambda_j)$. For M/M/1, this equals $p_j = \mu_j / (\mu_j - \Lambda_j)^2$. Each source then computes a best response by solving its local convex subproblem and applies a damped update. In our runs, we use $\eta = 0.3$, $\gamma = 0.5$, a maximum of 400 iterations, and we stop when $\|\lambda^{(t+1)} - \lambda^{(t)}\| / \|\lambda^{(t)}\| < 10^{-7}$.

B. Centralized Benchmark

The solver converges to an optimal objective value

$$F^* = 2.01575,$$

and terminates after 33 iterations. Table I reports the resulting service node utilizations, which are all strictly below 1, confirming stability at the optimum.

C. Distributed Pricing-Based Iteration

We next run the distributed pricing-based iteration in Algorithm 1 on the same static instance. The distributed method converges in 38 iterations and attains an objective value $F_{\text{dist}} = 2.01595$, compared to the centralized optimum $F^* = 2.01575$.

We declare convergence when the relative change in the routing matrix satisfies $\|\lambda^{(t+1)} - \lambda^{(t)}\|_F / \|\lambda^{(t)}\|_F \leq 10^{-7}$. The resulting service node utilizations are reported in Table I and closely match the centralized benchmark.

D. Convergence Behavior

We next examine the convergence behavior of the distributed pricing-based iteration. Figure 2 plots the objective value $F(\lambda^{(t)})$ across iterations. The objective decreases sharply during the first few iterations and then flattens as the iterates approach a steady operating point.

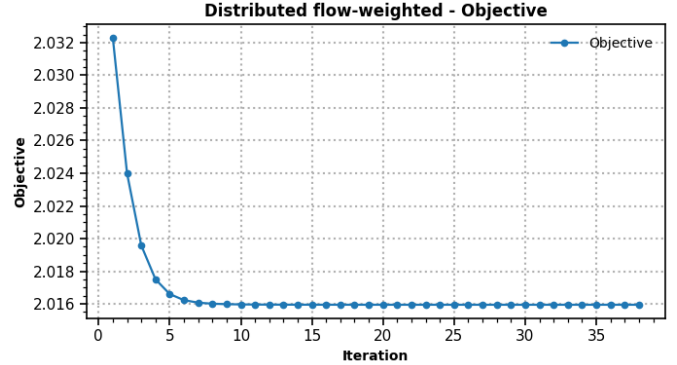


Fig. 2. Distributed flow-weighted: objective value $F(\lambda^{(t)})$ versus iteration.

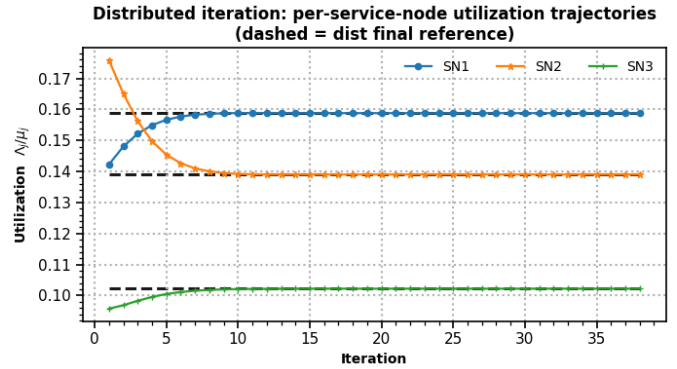


Fig. 3. Distributed pricing iteration: per-SN utilization trajectories $\Lambda_j^{(t)} / \mu_j$ over iterations (dashed = distributed final reference).

Figure 3 reports the per-SN utilization trajectories $\Lambda_j^{(t)} / \mu_j$ across distributed iterations. The utilizations exhibit a short transient and then stabilize as prices and source splits approach a fixed point. The dashed horizontal lines indicate the final distributed utilizations, showing that each SN's utilization converges to a steady-state value under the pricing updates.

Finally, Figure 4 plots the per-source flow-weighted mean end-to-end delay over the distributed pricing iterations, where each curve corresponds to one source and the delay is computed under the current split $\lambda^{(t)}$ as $\bar{D}_i^{(t)} \triangleq \sum_{j \in \mathcal{J}} \frac{\lambda_{ij}^{(t)}}{\lambda_i} (D_{ij}(\lambda_{ij}^{(t)}) + D_j(\Lambda_j^{(t)}))$. All sources exhibit a short transient followed by a stable plateau, indicating that the routing variables and induced congestion levels are settling to a steady operating point. The trajectories are monotone or nearly monotone after the first few iterations, with the largest change occurring early, consistent with the fast initial decrease in the global objective. The steady-state separation across sources reflects heterogeneity in their feasible access capacities $\{\mu_{ij}\}$ and the SN capacities $\{\mu_j\}$: some sources quickly converge to a lower mean delay (e.g., $P4$), while others remain at higher delay levels (e.g., $P3$), even at the converged allocation.

E. Solution Comparison to Centralized Optimum

We compare the distributed fixed point to the centralized system-optimal solution for the same static instance. The

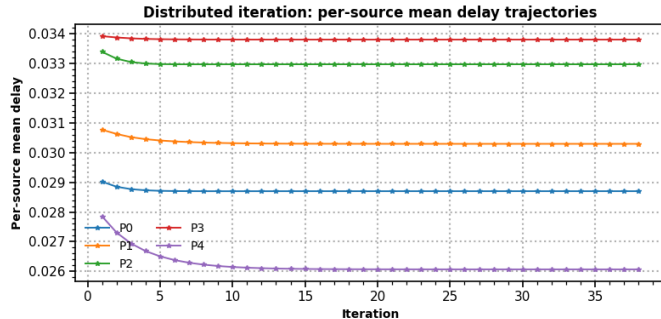


Fig. 4. Distributed pricing iteration: per-source mean delay trajectories versus iteration.

Solver	util _{SN1}	util _{SN2}	util _{SN3}
central_flow	0.158	0.139	0.103
dist_flow	0.159	0.139	0.102

TABLE I

THEORETICAL SOLVER UTILIZATIONS FOR THE STATIC SYSTEM (FLOW-WEIGHTED OBJECTIVE).

centralized solver attains an objective value $F^* = 2.01575$, while the distributed iteration converges to $F_{\text{dist}} = 2.01595$. The absolute objective gap is $F_{\text{dist}} - F^* = 2.005 \times 10^{-4}$, corresponding to a relative gap of approximately 9.95×10^{-5} .

Table I reports the service node utilizations Λ_j/μ_j under the centralized and distributed solutions. The utilizations match closely across all three service nodes, indicating that the pricing-based iteration reproduces the centralized load distribution to within a small numerical tolerance.

Figure 5 checks whether the centralized optimum and the distributed fixed point satisfy the Wardrop-type optimality structure in (14). For each source i , we compute the total marginal cost on every candidate route, $M_{ij} = C_{ij}(\lambda_{ij}) + C_j(\Lambda_j)$. At the centralized solution, the total marginal costs on all utilized routes for a given source are (nearly) equal, while routes not used by that source have no smaller total marginal cost. The distributed fixed point exhibits the same pattern: the routes carrying positive flow for each source align closely in total marginal cost, and unused routes are not cheaper in total marginal cost. Small residual deviations reported within each panel reflect numerical tolerance and the stopping criterion of the distributed iteration.

F. Stochastic M/M/1 Validation (Same Parameters)

We also run a lightweight stochastic M/M/1 simulation on the same static instance, where arrivals are Poisson and service times are exponential using the same source rates $\{\lambda_i\}$, access capacities $\{\mu_{ij}\}$, and service capacities $\{\mu_j\}$ as in the deterministic solvers. The purpose is only to sanity-check that time-domain queueing behavior is consistent with the steady-state operating point predicted by the centralized optimum and the distributed fixed point.

Figure 6 shows EWMA-smoothed SN utilization trajectories from the stochastic run, together with horizontal reference lines from the deterministic centralized and distributed

solutions. After a short transient, the stochastic utilization fluctuates around these reference levels. The centralized and distributed references are nearly identical, and the stochastic trajectories remain close to them, suggesting that the deterministic solutions provide a reasonable operating-point prediction for this instance.

Figure 7 compares the deterministic rate split induced by the distributed fixed point to the time-averaged split observed in the stochastic simulation. Across sources, the stochastic averages closely track the deterministic split, indicating that the distributed solution captures the steady-state allocation that emerges under stochastic queueing. Small deviations are consistent with finite-horizon averaging and stochastic variability, rather than a systematic shift in the underlying operating point.

In Figure 8, the per-source mean delays stabilize after the initial transient and exhibit bounded fluctuations driven by stochastic queueing. This time-domain view in the M/M/1 setting complements Fig. 4, which shows convergence of per-source mean delays over distributed iterations in the deterministic model.

Overall, the stochastic simulation stabilizes around the deterministic operating point and yields time-averaged behavior consistent with the distributed fixed point (and the centralized optimum when the two overlap). These results support using the deterministic convex optimum and its distributed realization as steady-state benchmarks under stochastic M/M/1 dynamics.

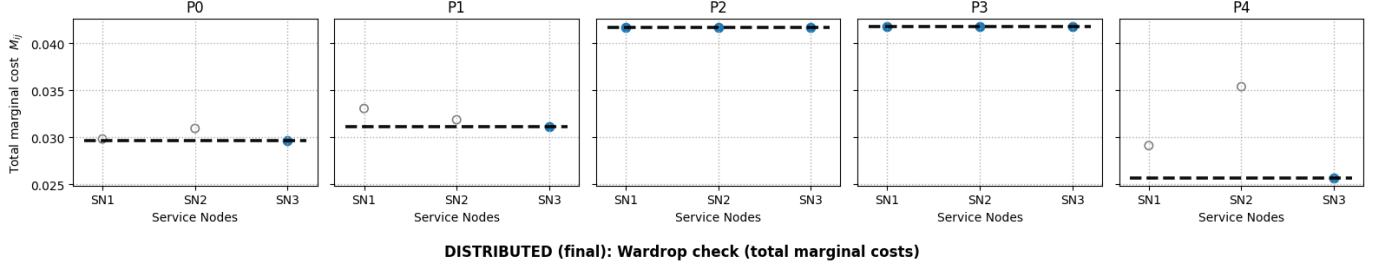
G. Discussion

These illustrative results support two main points. First, for a static instance with both access congestion and server congestion, the distributed pricing-based iteration converges reliably and produces an objective value close to the centralized optimum. Second, the resulting service node utilizations closely match the centralized benchmark, suggesting that the decentralized updates recover the same load-splitting structure implied by the KKT marginal-cost equalization.

VII. CONCLUSION

We studied a steady-state multi-source traffic allocation problem in which end-to-end delay is driven jointly by rate-dependent, capacity-constrained access-path delays and load-dependent queueing delays at capacity-constrained service nodes. Under standard monotonicity and convexity assumptions, the resulting flow-weighted delay minimization is a convex program, enabling a global system-optimal characterization via KKT conditions with a Wardrop-type total marginal cost equalization interpretation. Leveraging this structure, we developed a lightweight distributed pricing-based algorithm in which service nodes compute and broadcast scalar congestion prices from locally observed aggregate loads, while sources update their traffic splits by solving small separable convex allocation problems under the advertised prices, and numerical illustrations demonstrated convergence to the centralized optimum.

CENTRAL optimum: Wardrop check (total marginal costs)



DISTRIBUTED (final): Wardrop check (total marginal costs)

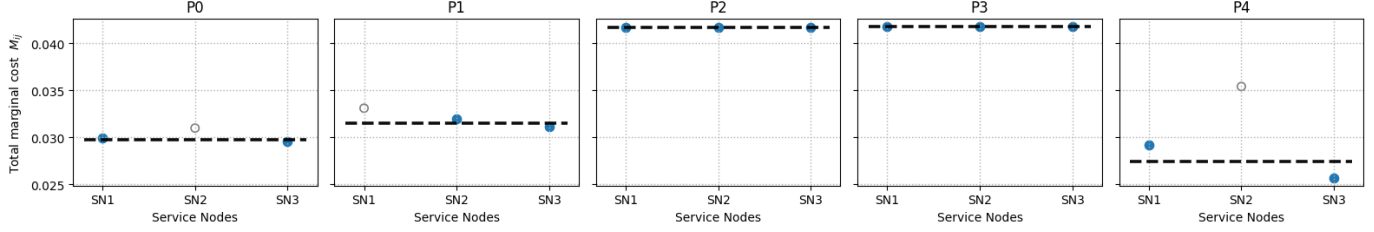


Fig. 5. Wardrop (KKT) check via total marginal costs $M_{ij} = C_{ij}(\lambda_{ij}) + C_j(\Lambda_j)$. For each source, all *used* routes (filled markers) align closely in total marginal cost, while *unused* routes (hollow markers) have no smaller cost, consistent with (14). Top: centralized optimum. Bottom: distributed fixed point, showing the same marginal-cost equalization pattern.

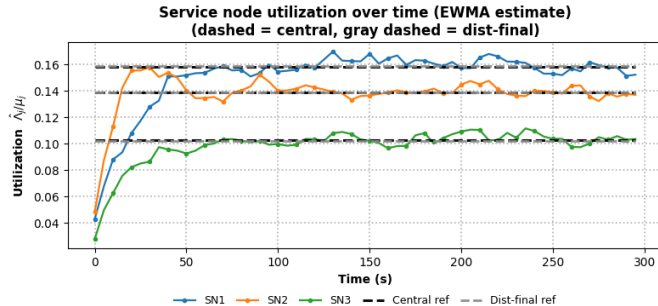


Fig. 6. Stochastic M/M/1 simulation: SN utilization over time (EWMA estimate). Dashed reference lines indicate deterministic utilizations from the centralized optimum and the distributed fixed point.

Future directions include analyzing fully asynchronous implementations with delayed or stale price information, extending the model to time-varying capacities and nonstationary operating regimes. Future work could also compare the proposed capacity-aware optimization framework against capacity-unaware but queue-aware control policies, including Lyapunov drift-plus-penalty (backpressure) methods, to quantify performance and robustness trade-offs across regimes. Another promising direction is to explore reinforcement learning and multi-agent reinforcement learning approaches that learn effective load allocation policies from data or trial-and-error in a given network/server environment, as an alternative to the proposed model-based optimization, as well as hybrid model-data-driven methods that combine structural insights from convexity and marginal-cost pricing with learned components to improve adaptability under uncertainty. **The source code for the algorithms and their simulations are publicly**

available at . The repository includes additional results from the Python implementation of joint network-and-server congestion routing: KKT/Wardrop checks, convergence plots, and stochastic validation.

REFERENCES

- [1] R. G. Gallager, “A minimum delay routing algorithm using distributed computation,” *IEEE Transactions on Communications*, vol. 25, no. 1, pp. 73–85, 1977.
- [2] F. P. Kelly, A. K. Maulloo, and D. K. Tan, “Rate control for communication networks: shadow prices, proportional fairness and stability,” *Journal of the Operational Research Society*, vol. 49, no. 3, pp. 237–252, 1998.
- [3] S. H. Low and D. E. Lapsley, “Optimization flow control. i. basic algorithm and convergence,” *IEEE/ACM Transactions on Networking*, vol. 7, no. 6, pp. 861–874, 1999.
- [4] T. Rambha, S. D. Boyles, and P. Stone, “Marginal cost pricing for system optimal traffic assignment with recourse under supply-side uncertainty,” *Transportation Research Part B: Methodological*, vol. 110, pp. 104–131, 2018.
- [5] D. Paccagnan, B. Gentile, F. Parise, M. Kamgarpour, and J. Lygeros, “Nash and wardrop equilibria in aggregative games with coupling constraints,” *IEEE Transactions on Automatic Control*, vol. 64, no. 4, pp. 1373–1388, 2019.
- [6] D. Q. Vu, K. Antonakopoulos, and P. Mertikopoulos, “Fast routing under uncertainty: Adaptive learning in congestion games with exponential weights,” in *Advances in Neural Information Processing Systems (NeurIPS)*, 2021. [Online]. Available: <https://proceedings.neurips.cc/paper/2021/file/7b86f36d139d8581d4b5a4f155ba431c-Paper.pdf>
- [7] V.-D. Nguyen *et al.*, “Network-aided intelligent traffic steering in 6g o-ran: A multi-layer optimization framework,” *IEEE Transactions on Mobile Computing*, 2024.
- [8] A. Habib *et al.*, “Traffic steering for 5g multi-rat deployments using deep reinforcement learning,” *arXiv preprint arXiv:2301.05316*, 2023.
- [9] M. Mitzenmacher, “The power of two choices in randomized load balancing,” *IEEE Transactions on Parallel and Distributed Systems*, vol. 12, no. 10, pp. 1094–1104, 2001.
- [10] Y. Lu *et al.*, “Join-idle-queue: A novel load balancing algorithm for dynamically scalable web services,” *Performance Evaluation*, vol. 68, no. 11, pp. 1056–1071, 2011.

Rate split comparison (Distributed vs stochastic average)

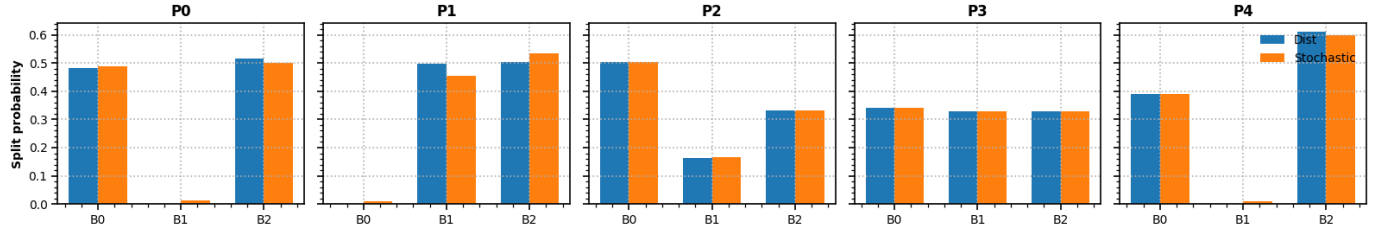


Fig. 7. Rate split comparison: distributed fixed-point routing fractions versus time-averaged stochastic routing fractions (per source across service nodes).

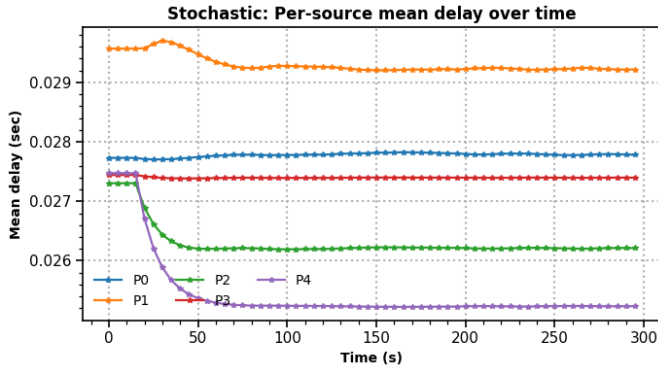


Fig. 8. Stochastic M/M/1 simulation: per-source mean end-to-end delay versus time.

- [11] M. A. Qureshi, Y. Cheng, Q. Yin, Q. Fu, G. Kumar, M. Moshref, J. Yan, V. Jacobson, D. J. Wetherall, and A. Kabbani, “Plb: Congestion signals are simple and effective for network load balancing,” in *Proceedings of the ACM SIGCOMM 2022 Conference (SIGCOMM '22)*. Amsterdam, Netherlands: ACM, 2022, pp. 207–218.
- [12] S. Balseiro *et al.*, “Load balancing with network latencies via distributed gradient descent,” *arXiv preprint arXiv:2504.10693*, 2025.
- [13] R. Urgaonkar *et al.*, “Dynamic service migration and workload scheduling in edge-clouds,” *Performance Evaluation*, vol. 91, pp. 205–228, 2015.
- [14] D. T. Nguyen, L. B. Le, and V. Bhargava, “Price-based resource allocation for edge computing: A market equilibrium approach,” *IEEE Transactions on Cloud Computing*, vol. 9, no. 1, pp. 302–317, 2021.